



Plasma-Enhanced ALD of TiO₂ Thin Films on SUS 304 Stainless Steel for Photocatalytic Application

Chang-Soo Lee,^a Jungwon Kim,^b J. Y. Son,^a W. J. Maeng,^a Du-Hwan Jo,^c
Wonyong Choi,^b and Hyungjun Kim^{a,*z}

^aDepartment of Materials Science and Engineering and ^bSchool of Environmental Science and Engineering, Pohang University of Science and Technology, Pohang 790-784, Korea

^cSurface Technology Research Group, POSCO Technical Research Laboratories, Gwangyang 545-090, Korea

Plasma-enhanced atomic layer deposition (PE-ALD) of TiO₂ thin films using Ti(NMe₂)₄ [tetrakis(dimethylamido) Ti] and O₂ plasma were prepared on stainless steel to show the self-cleaning effect. The TiO₂ thin films deposited on stainless steel have high growth rate, large surface roughness, and low impurities. The film deposited below 200°C was amorphous, while the films deposited at 300 and 400°C showed anatase and rutile phases, respectively. The contact angle measurements on crystalline PE-ALD TiO₂ thin films exhibited superhydrophilicity after UV irradiation. The TiO₂ thin film with anatase phase deposited at 300°C showed the highest photocatalytic efficiency, which is higher than on Activ glass or thermal ALD TiO₂ films. We suggest that anatase structure and large surface area of TiO₂ thin film on stainless steel are the main factors for the high photocatalytic efficiency.

© 2009 The Electrochemical Society. [DOI: 10.1149/1.3095515] All rights reserved.

Manuscript submitted December 16, 2008; revised manuscript received February 9, 2009. Published March 19, 2009.

Since photoinduced water splitting on titanium dioxide (TiO₂) electrode was discovered,¹ TiO₂ has been regarded as one of the most promising photocatalytic materials due to its high photocatalytic activity, high chemical stability, low toxicity, and low cost. As a photocatalyst, when UV light with higher energy than the bandgap of TiO₂ is illuminated, electron-hole pairs are generated in the TiO₂ films. The photogenerated holes in the valence band and the electrons in the conduction band diffuse to the TiO₂ surface and they produce highly energetic hydroxyl radicals ([•]OH) and superoxide radical anions (O₂^{•-}) which can oxidize organic molecules on the TiO₂ surface.^{2,4} In addition, TiO₂ photocatalyst kills bacteria^{5,6} and induces a hydrophilic surface after UV irradiation.^{7,8} Thus, TiO₂ photocatalysts are widely used in various fields, such as window glass, ceramic tiles, and wall papers utilizing its self-cleaning,^{9,10} antifogging,^{7,8} antibacterial activities,^{5,6} and water or air purification.^{11,12}

Two different tetragonal phases of TiO₂, anatase and rutile, are commonly used in photocatalysis. The structures of both anatase and rutile consist of chains of TiO₆ octahedra, but lattice structures of two crystals are obviously different.¹³ The differences in lattice structure cause different mass densities (3.894 g/cm³ for anatase and 4.250 g/cm³ for rutile) and electronic bandgaps (3.3 eV for anatase and 3.1 eV for rutile). The anatase phase has a more negative conduction band edge potential (higher potential energy of photogenerated electrons) than the rutile phase, so it is well known that the photocatalytic activities of the anatase phase are superior to those of the rutile phase.³ Thus, in terms of photocatalytic efficiency, obtaining a suitable crystalline phase and high specific area are important factors.

For practical applications, it is necessary to deposit TiO₂ thin films on various solid substrates such as glass, ceramic tiles, and steel. There are several reports about the TiO₂ photocatalyst on glass^{9,14-17} and ceramic tiles^{18,19} to give the surface of these materials a self-cleaning effect utilizing the photocatalytic effect. Also, commercial products such as Activ glass produced by Pilkington Corp. are being used for building windows. While the TiO₂ coating on steel substrate is still in the early stage of development compared to coatings on glass, steel has benefits as a substrate for photocatalysis, such as good workability originating from its ductility, that glass and ceramic tiles do not have, and has a high specific surface area originating from its large surface roughness which can enhance pho-

tocatalytic efficiency. Thus, TiO₂ photocatalyst on steel can be used in many applications such as automobile bodies, hospital equipment, and kitchen appliances to keep their surfaces clean in open spaces. Recently, Yang et al. reported that TiO₂ thin films deposited on steel showed higher photocatalytic efficiency than other substrates including Si and glass.²⁰

There have been many reports on the deposition of TiO₂ as photocatalyst using various methods including sol-gel,²¹ spray pyrolysis,²² hydrothermal synthesis,²³ sputtering,¹⁶ chemical vapor deposition,²⁴ pulsed laser deposition,²⁵ and atomic layer deposition (ALD).^{14,26} ALD is characterized by the alternate exposure of chemical species with self-limiting surface reactions. Thus, ALD has several advantages over other deposition methods such as good film quality, accurate thickness control, excellent conformality, and uniformity over large areas. Recently, several research groups reported on the ALD process of TiO₂ thin films on stainless steel and their photocatalytic activity²⁷ and anticorrosion activities.²⁸ Meanwhile, plasma-enhanced ALD (PE-ALD) has more benefits than thermal ALD due to its improved film properties, high growth rate, and the possibility of deposition at reduced substrate temperatures. Thus, it can be a very effective method for the preparation of TiO₂ thin films on steel, which has a highly rough surface and needs large area uniformity. However, the PE-ALD process of TiO₂ thin films on stainless steel has rarely been studied for the application of photocatalytic effects. Because high growth rate, reduced deposition temperature, and the control of deposited phase with mass production compatibility are potentially important considerations for the TiO₂ photocatalysis coatings on commercial products such as stainless steel, glass, and ceramic tile, it is necessary to investigate the photocatalytic effects of PE-ALD TiO₂ for higher productivity and cost savings.

In our previous report, we investigated the thermal and PE-ALD process of TiO₂ thin films on Si(001) from an alkylamide precursor, Ti(NMe₂)₄ [tetrakis(dimethylamido) Ti, TDMAT] using water and oxygen plasma, respectively, and analyzed their microstructure, chemical composition, and electrical properties.²⁹ In this study, we investigated the PE-ALD process of TiO₂ thin films on SUS 304 austenitic stainless steels and their structural properties based on our previous research. We especially focused on the self-cleaning effects of PE-ALD TiO₂ by measuring photoinduced hydrophilicity using contact-angle measurement of water and photocatalytic activity of TiO₂ thin films by decomposition of organic liquid such as 4-chlorophenol. The photocatalytic effects of PE-ALD TiO₂ thin films on stainless steel were better than that of Activ glass and thermal ALD TiO₂ thin films.

* Electrochemical Society Active Member.

^z E-mail: hyungjun@postech.ac.kr

Experimental

A homemade coldwall-type remote PE-ALD chamber was used to deposit TiO₂ thin films. Sample size up to 200 mm in diameter can be loaded into the chamber, which is pumped by a turbomolecular pump with the base pressure in the range of middle 10⁻⁶ Torr. The substrates were heated using a resistive heating plate, providing temperatures up to around 500°C, which was measured by a thermocouple attached to the heater. TDMAT and O₂ plasma were used as a Ti precursor and O reactant, respectively. Because the TDMAT has high enough vapor pressure, the bubbler was kept at room temperature without the use of carrier gas. The flow of oxygen controlled by a mass flow controller was set at 20 sccm, resulting in 10 mTorr of working pressure, and the plasma power was 300 W. The chamber was purged by 50 sccm Ar gas between the precursor and the reactant exposure step.

TiO₂ thin films were deposited on 15 × 15 mm Si(001) and SUS 304 austenitic stainless steel sheets. Before being loaded into the chamber, Si(001) substrates were cleaned by rinsing in acetone, isopropyl alcohol, and then in deionized (DI) water, while SUS 304 stainless steel substrates were cleaned in an ultrasonic bath sequentially using acetone, ethanol, and DI water separately. Then both Si and SUS 304 stainless steel were dried with N₂ gas. The growth temperatures were 150, 200, 300, and 400°C. The PE-ALD growth sequence consists of a 1.5 s pulse of TDMAT, 5 s of Ar purge, 3 s pulse of O₂ plasma, and 5 s of Ar purge. The PE-ALD growth sequence was repeated for 500 cycles. After deposition, the thickness was measured by ellipsometry and field-emission scanning electron microscopy. The impurity content and binding structure of the films were analyzed by X-ray photoemission spectroscopy (XPS). The crystal structures were determined by a glancing-angle X-ray diffraction (XRD) with 1° angle of incident for all samples. Atomic force microscopy (AFM) was used to investigate the surface morphology and the surface roughness of the films.

To investigate the self-cleaning effects of the TiO₂ thin films on stainless steel, we measured the contact angle of water on steel surface and photoinduced degradation of organic liquid as a function of UV exposure time. In these experiments, we used Pilkington Activ glass for comparison. For the measurement of contact angle, a black light blue lamp (10 W, wavelength 350–400 nm) was used as a light source and the exposure time range was 3–120 min. To analyze photocatalytic activity, the degradation rates of 4-CP were monitored. The initial concentration of 4-CP was 0.1 mM, and TiO₂ thin films were exposed with a 300 W Xe arc lamp (Oriental) as a light source. Light passes through an IR filter and UV cutoff filter ($\lambda > 324$ nm), and then the filtered light is focused onto an 11 mL Pyrex reactor. Upon UV irradiation, samples were withdrawn by a 1 mL syringe. Identification and quantification of 4-CP were performed by using high-performance liquid chromatography.

Results and Discussion

In order to obtain a growth condition of TiO₂ films by PE-ALD, both Si(001) and stainless steel substrate were used to deposit TiO₂ thin films. For the PE-ALD TiO₂ process from TDMAT and O₂ plasma, we obtained TiO₂ thin films with a thickness around 120 nm on both substrates. The growth rate of PE-ALD TiO₂ films was 2.5 Å/cycle on both Si(001) and stainless steel, which was much higher than the previously reported values from other precursors including methoxide (0.6 Å/cycle)¹⁴ and chloride (0.5 Å/cycle).^{27,30} These films have nearly similar growth rate for all deposition temperatures, and the thickness of films increased with increasing ALD cycles. From these results, we confirm that TiO₂ thin film on Si(001) and stainless steel substrates was grown by ALD.

Figure 1a and b shows the XRD patterns of the TiO₂ thin films depending on growth temperatures on the Si(001) and stainless steel substrates, respectively. The crystal structure of TiO₂ films exhibits strong dependency on the deposition temperature on both substrates. The films grown at deposition temperatures below 200°C were

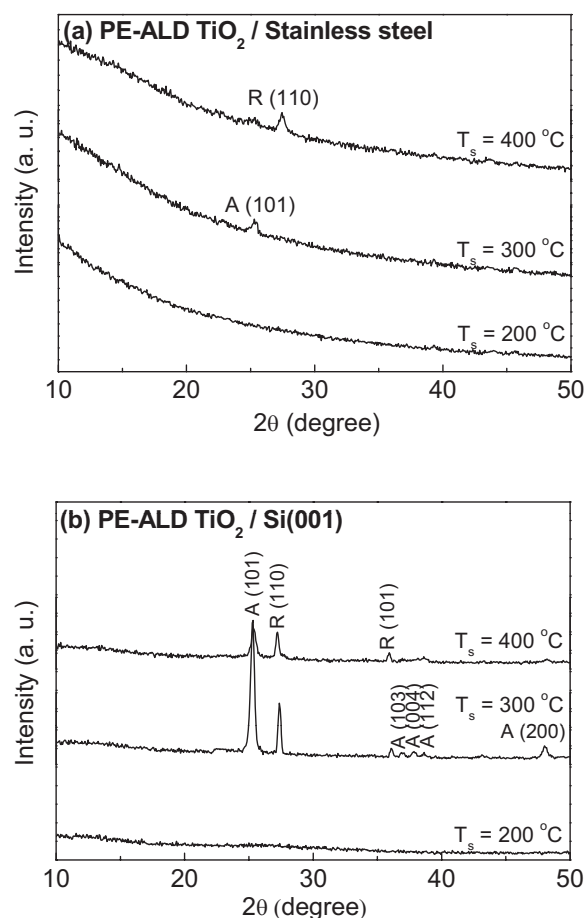


Figure 1. XRD patterns of PE-ALD TiO₂ thin films (a) on stainless steel and (b) on Si(001) as a function of growth temperature.

amorphous on both substrates, judging from the absence of any diffraction peaks. TiO₂ thin film on Si(001) substrate showed a mixture of anatase and rutile phases for both deposition temperatures of 300 and 400°C, while the thin films on stainless steel substrate showed anatase and rutile phases for the deposition temperatures of 300 and 400°C, respectively. Namely, the crystal structures of TiO₂ thin films changed from amorphous to anatase and rutile phase with increasing growth temperature. Similar XRD results were reported for ALD TiO₂ thin film from TiI₄ and H₂O₂ by Kukli et al.³¹ They reported that ALD TiO₂ films grown at temperatures around 300°C had anatase phase or a mixture of anatase and rutile phases, while films grown at 425°C had only rutile phase. However, for ALD TiO₂ films from TiCl₄ and water vapor, the films deposited at 400°C had only anatase phase.³²

To analyze the chemical composition and the binding structure, we obtained XPS spectra for the PE-ALD TiO₂ thin films on Si(001) and stainless steel substrates. Figure 2a-c presents the spectrum of the TiO₂ thin film deposited at 300°C on both substrates. The XPS spectrum of Ti 2p, O 1s, and N 1s levels for TiO₂ thin films on both substrates showed a similar trend, as seen in Fig. 2a-c. Only pure Ti–O bond-related XPS peaks were observed at Ti 2p_{2/3} (located at 458.8 eV) and Ti 2p_{1/2} (located at 464.3 eV), which have a peak separation of 5.5 eV. These results indicated the presence of Ti⁴⁺ in these films and no existence of Ti–N compound and metallic Ti. From the O 1s spectra, two O-related peaks are observed. The peak at 530.1 eV is associated with pure TiO₂, and the shoulder around 531.7 eV is attributed to the O in the OH group.^{33,34} The N 1s spectrum in Fig. 2c shows no signal related to nitrogen, in spite of

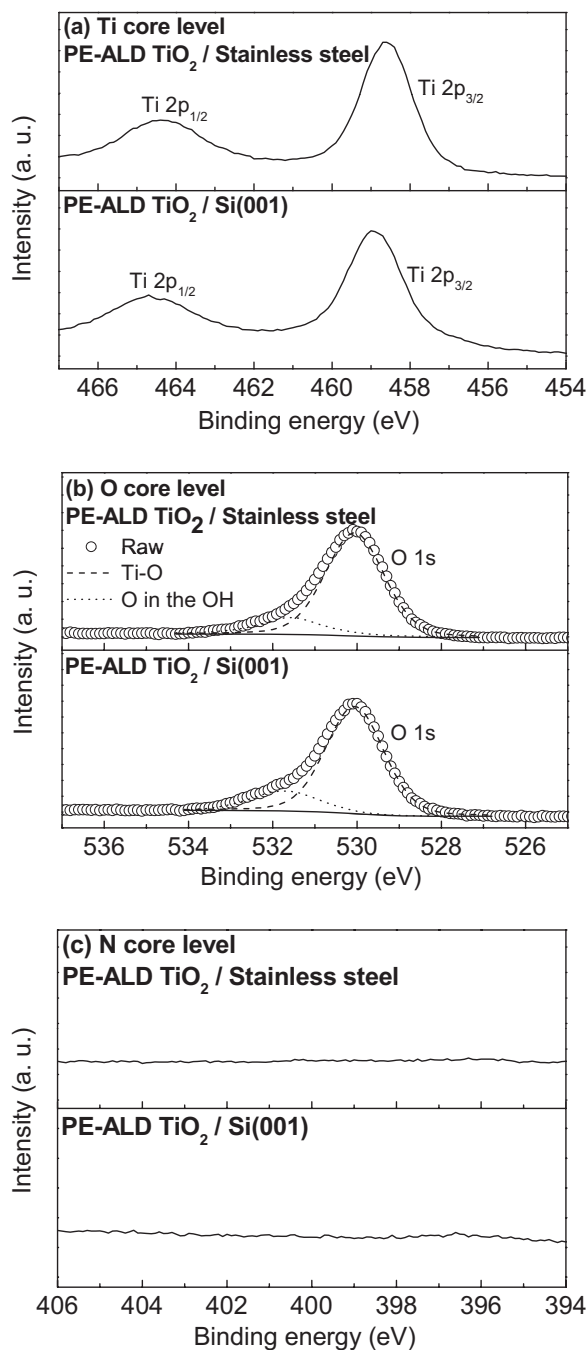


Figure 2. XPS data for (a) Ti 2p, (b) O 1s, and (c) N 1s of the PE-ALD TiO₂ thin films on stainless steel and Si(001) deposited at 300°C.

using amide precursor for the current experiments. Thus, we inferred that the TiO₂ thin films on both Si(001) and stainless steel substrates are quite pure.

The XRD and XPS results show that TiO₂ thin films with polycrystalline phases and low impurities are deposited on the stainless steel as well as on Si at $T_s = 300\text{--}400^\circ\text{C}$. Then we compared the surface roughness, contact angle of water, and degradation rate of organic liquid of TiO₂ thin films on stainless steel with Pilkington Activ glass to investigate the photocatalytic effects. AFM images of TiO₂-coated stainless steel and Pilkington Activ glass are shown in Fig. 3. The surface roughnesses of PE-ALD TiO₂ thin films on stainless steel and glass substrates are around 55.4 and 6.3 nm, respectively. From this result, we inferred that TiO₂ thin films on

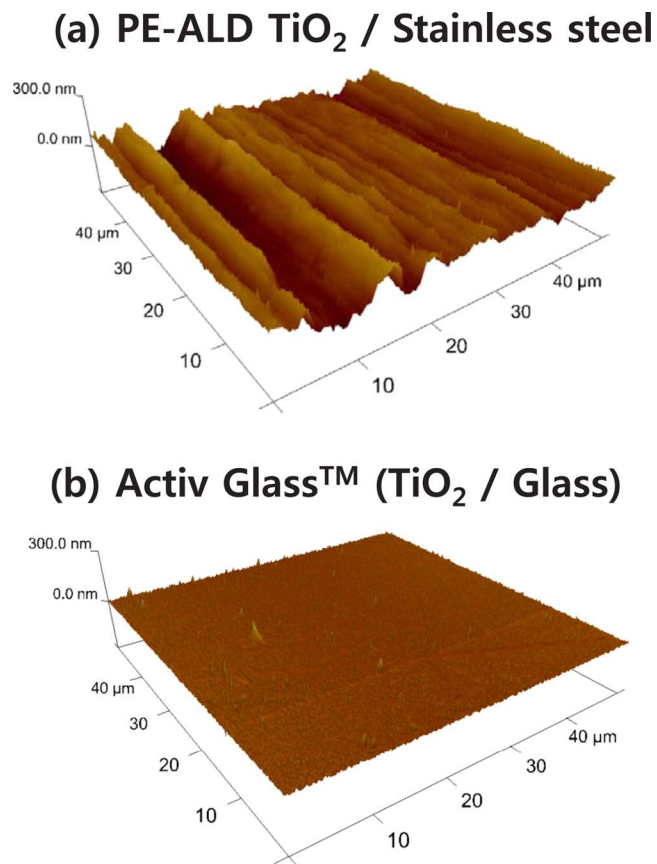


Figure 3. (Color online) AFM images of TiO₂ thin films (a) on stainless steel and (b) on glass.

stainless steel have a larger surface area than Activ glass, which affects the higher photocatalytic efficiency of TiO₂ thin films on stainless steel.

Figure 4 shows the contact angle of water on the TiO₂ thin films as a function of UV exposure time. The initial contact angle of amorphous TiO₂ thin film is about 62°, while those of anatase and rutile TiO₂ thin films and Activ glass are about 26, 16, and 45°, respectively. After the exposure of UV light for 2 h, the amorphous TiO₂ thin film shows a small change of about 6° in contact angle. The contact angles of anatase and rutile TiO₂ thin films gradually

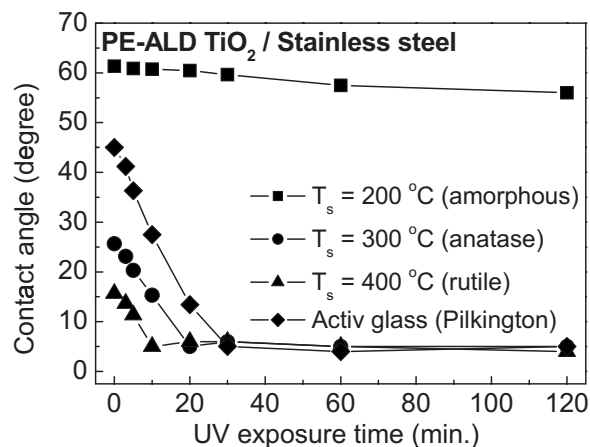


Figure 4. Contact angles of water on TiO₂ thin films deposited at each growth temperature as a function of UV irradiation time.

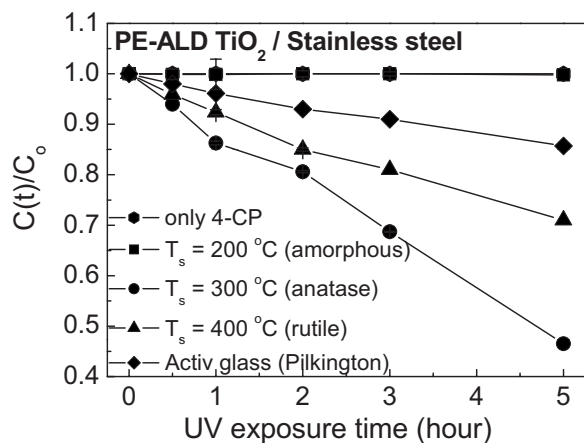


Figure 5. Decomposition of 4-CP for TiO₂ thin films at each growth temperature as a function of UV irradiation time.

decrease and finally approach 5° after the exposure time of 20 min. The contact angle of Activ glass also gradually decreases and finally approaches 5° after 30 min of UV irradiation. Thus, the Activ glass and polycrystalline PE-ALD TiO₂ thin films with anatase and rutile structures have a superhydrophilic surface, which can provide various advantages such as antifogging and self-cleaning effects.

There are several studies on the superhydrophilicity of TiO₂ thin films.^{7,8,35} Takaoka et al.³⁶ reported similar results from TiO₂ thin films with polycrystalline phases by an O₂ cluster ion-beam-assisted deposition method. They showed that only the polycrystalline TiO₂ thin film had a superhydrophilic surface after UV light exposure. The mechanism of hydrophilicity is different from that of photocatalytic activity, although the photogenerated electrons and holes are involved in both cases. Wang et al.⁷ reported that the surface hydrophilicity of anatase and rutile TiO₂ thin films is independent of their photocatalytic activities, and they explained that this effect occurs due to the production of oxygen vacancies on the TiO₂ surface during the exposure of UV light. After electron-hole pairs are generated during UV exposure, the electrons reduce the Ti(IV) cations to Ti(III) states and the holes oxidize O₂ anions. In this process, oxygen atoms are ejected from TiO₂ surface and oxygen vacancies are created. Then these oxygen vacancies are expected to interact strongly with water molecules and they occupy oxygen vacancies, producing adsorbed OH groups which were attributed to the hydrophilicity of the TiO₂ surface. They observed the wettability change on both the anatase and rutile TiO₂ surface of polycrystals or single crystals independent of their photocatalytic activities. Our results are consistent with these results that photoinduced superhydrophilicity was observed on TiO₂ thin films with anatase and rutile phases.

To estimate the photocatalytic effects, the decomposition rates of 4-CP were measured under UV irradiation. Figure 5 shows the concentration variation of 4-CP liquid as a function of UV exposure time. For only 4-CP liquid and the amorphous TiO₂ thin film, no decomposition of 4-CP is observed after the exposure of UV light. However, noticeable concentration decrease of 4-CP is observed for the polycrystalline TiO₂ thin films with anatase, rutile phases, and Pilkington Activ glass. They decomposed 4-CP aqueous solution, showing a concentration decrease of about 55, 30, and 15%, respectively, after 5 h UV irradiation. The highest photocatalytic activity of TiO₂ thin films was obtained for anatase TiO₂ thin film on stainless steel, which was deposited at 300°C.

This result indicates that the crystal structure of TiO₂ thin films is one of the most important factors to improve the photocatalytic efficiency of TiO₂. As mentioned above, anatase phase of TiO₂ which has a more negative conduction band edge potential (higher potential energy of photogenerated electrons) than the rutile phase, shows higher photocatalytic activities than rutile TiO₂. From our

results, we observed that anatase TiO₂ thin film had higher photocatalytic activities than those of the films with rutile phase or a mixture of anatase and rutile phase. Moreover, we inferred that the large surface area of TiO₂ thin films on stainless steel enhances the decomposition rate of organic liquid compared to Activ glass. We suggest that the higher photocatalytic efficiency of anatase TiO₂ thin film than that of rutile TiO₂ thin film and Activ glass originated from a suitable phase of TiO₂ thin film and larger surface area of the film on stainless steel. For comparison, we also measured the photocatalytic effects of thermal ALD TiO₂ thin films on stainless steel deposited using TDMAT and H₂O at 300°C, which is a polycrystalline TiO₂ with both anatase and rutile phases. The thermal ALD TiO₂ thin film has shown about 30% decrease of 4-CP concentration for 5 h UV irradiation (data not shown). Thus, PE-ALD has a potential benefit compared to thermal ALD in terms of photocatalytic effect, mainly due to the greater degree of freedom in controlling deposited phase in the film.

Conclusions

TiO₂ thin films were deposited on steel substrate by PE-ALD from TDMAT and O₂ plasma, which exhibited relatively high growth rate and low impurity. The crystal structure of TiO₂ films depends on the growth temperatures. The anatase and rutile TiO₂ thin films were deposited at growth temperatures of 300 and 400°C, respectively. From AFM analysis, TiO₂ thin films on stainless steel have larger surface area due to large surface roughness than Activ glass. The contact angle of water and the decomposition of 4-CP after UV irradiation were measured to confirm the self-cleaning effect of TiO₂ thin films on stainless steel. A commercial product, Activ glass, was also used to measure the contact angle of water and the decomposition of 4-CP for comparison. Activ glass and TiO₂ thin films with anatase and rutile phases on stainless steel showed superhydrophilic phenomena and decomposed 4-CP after UV irradiation. The anatase TiO₂ thin film on stainless steel showed the highest photocatalytic activity after 5 h UV irradiation. We suggest that the highest photocatalytic efficiency of TiO₂ thin film with anatase structure is attributed to its suitable phase and large surface area.

Acknowledgments

This work was supported by POSCO Technical Research Laboratories, Blue Ocean Technology project (2008Y233). One of the authors (C. S. Lee) was financially supported by the second stage of the Brain Korea project in 2008.

Pohang University of Science and Technology assisted in meeting the publication costs of this article.

References

1. A. Fujishima and K. Honda, *Nature (London), New Biol.*, **238**, 37 (1972).
2. A. Heller, *Acc. Chem. Res.*, **28**, 503 (1995).
3. A. Fujishima, T. N. Rao, and D. A. Tryk, *J. Photochem. Photobiol. C*, **1**, 1 (2000).
4. C. Kormann, D. W. Bahnemann, and M. R. Hoffmann, *Environ. Sci. Technol.*, **25**, 494 (1991).
5. K. Sunada, Y. Kikuchi, K. Hashimoto, and A. Fujishima, *Environ. Sci. Technol.*, **32**, 726 (1998).
6. P.-C. Maness, S. Smolinski, D. M. Blake, Z. Huang, E. J. Wolfrum, and W. A. Jacoby, *Appl. Environ. Microbiol.*, **65**, 4094 (1999).
7. R. Wang, K. Hashimoto, A. Fujishima, M. Chikuni, E. Kojima, A. Kitamura, M. Shimohigoshi, and T. Watanabe, *Nature (London)*, **388**, 431 (1997).
8. R. Wang, K. Hashimoto, A. Fujishima, M. Chikuni, E. Kojima, A. Kitamura, M. Shimohigoshi, and T. Watanabe, *Adv. Mater. (Weinheim, Ger.)*, **10**, 135 (1998).
9. Y. Paz, Z. Lou, L. Rabenberg, and A. Heller, *J. Mater. Res.*, **10**, 2842 (1995).
10. Y. Ohko, S. Saitoh, T. Tatsuma, and A. Fujishima, *J. Electrochem. Soc.*, **148**, B24 (2001).
11. J. Peral, X. Domenech, and D. F. Ollis, *J. Chem. Technol. Biotechnol.*, **70**, 117 (1997).
12. J. A. Byrne, B. R. Eggins, N. M. D. Brown, B. McKinney, and M. Rouse, *Appl. Catal., B*, **17**, 25 (1998).
13. A. L. Linsebigler, G. Lu, and J. T. Yates, Jr., *Chem. Rev. (Washington, D.C.)*, **95**, 735 (1995).
14. V. Pore, A. Rahtu, M. Leskelä, M. Ritala, T. Sajavaara, and J. Keinonen, *Chem. Vap. Deposition*, **10**, 143 (2004).
15. T. Watanabe, A. Nakajima, R. Wang, M. Minabe, S. Koizumi, A. Fujishima, and K.

- Hashimoto, *Thin Solid Films*, **351**, 260 (1999).
16. S. Takeda, S. Suzuki, H. Odaka, and H. Hosono, *Thin Solid Films*, **392**, 338 (2001).
 17. T. Watanabe, S. Fukayama, M. Miyauchi, A. Fujishima, and K. Hashimoto, *J. Sol-Gel Sci. Technol.*, **19**, 71 (2000).
 18. P. S. Marcos, J. Marto, T. Trindade, and J. A. Labrincha, *J. Photochem. Photobiol., A*, **197**, 125 (2008).
 19. S. Kato, S. Kato, H. Taoda, and S. Katoh, *High Press. Res.*, **20**, 415 (2001).
 20. J.-L. Yang, Y. Li, F. Wang, Z.-G. Zang, and S.-J. Li, *J. Iron Steel Res. Int.*, **13**, 62 (2006).
 21. J. Yu, X. Zhao, and Q. Zhao, *Thin Solid Films*, **379**, 7 (2000).
 22. M. O. Abou-Helal and W. T. Seeber, *Appl. Surf. Sci.*, **195**, 53 (2002).
 23. J. H. Lee, M. Kang, S.-J. Choung, K. Ogino, S. Miyata, M.-S. Kim, J.-Y. Park, and J.-B. Kim, *Water Res.*, **38**, 713 (2004).
 24. A. Mills, N. Elliott, I. P. Parkin, S. A. O'Neill, and R. J. Clark, *J. Photochem. Photobiol., A*, **151**, 171 (2002).
 25. Y. Suda, H. Kawasaki, T. Ueda, and T. Ohshima, *Thin Solid Films*, **453-54**, 162 (2004).
 26. R. Pheamhom, C. Sunwoo, and D.-H. Kim, in *Characteristics of Atomic Layer Deposited TiO₂ Films and their Photocatalytic Activity*, p. 1535, American Vacuum Society, New York (2006).
 27. H. Kawakami, R. Ilola, L. Straka, S. Papula, J. Romu, H. Hanninen, R. Mahlberg, and M. Heikkila, *J. Electrochem. Soc.*, **155**, C62 (2008).
 28. C. X. Shan, X. Hou, and K.-L. Choy, *Surf. Coat. Technol.*, **202**, 2399 (2008).
 29. W. J. Maeng and H. Kim, *Electrochem. Solid-State Lett.*, **9**, G191 (2006).
 30. H. E. Cheng and C. C. Chen, *J. Electrochem. Soc.*, **155**, D604 (2008).
 31. K. Kukli, M. Ritala, M. Schuisky, M. Leskelä, T. Sajavaara, J. Keinonen, T. Untstare, and A. Härsta, *Chem. Vap. Deposition*, **6**, 303 (2000).
 32. H. E. Cheng, W. J. Lee, C. M. Hsu, M. H. Hon, and C. L. Huang, *Electrochem. Solid-State Lett.*, **11**, D81 (2008).
 33. C. N. Sayers and N. R. Armstrong, *Surf. Sci.*, **77**, 301 (1978).
 34. F. Zhao, X. Cui, B. Wang, and J. G. Hou, *Appl. Surf. Sci.*, **253**, 2785 (2006).
 35. A. Fujishima, T. N. Rao, and D. A. Tryk, *Electrochim. Acta*, **45**, 4683 (2000).
 36. G. H. Takaoka, M. Kawashita, K. Omoto, and T. Terada, *Nucl. Instrum. Methods Phys. Res. B*, **232**, 200 (2005).